Automatic Emergency Braking Sensor Configuration Effect on the Detection of U.S. Pedestrians

Samantha H. Haus, Rini Sherony, Hampton C. Gabler

Abstract Automatic Emergency braking (AEB) systems have the potential to mitigate or avoid vehicle-pedestrian crashes, if they can detect pedestrians with sufficient time to take evasive action. The objective of this study was to examine the effect of AEB sensor field-of-view (FOV) and range on the detection of pedestrians in real-world US vehicle-pedestrian crashes. This study utilized vehicle-pedestrian crashes from the Pedestrian Crash Data Study (PCDS). PCDS crash scene diagrams were manually digitized in AutoCAD and reconstructed to create vehicle and pedestrian trajectories. The crashes were then simulated with various AEB sensor systems to estimate each sensor system's pedestrian detection ability. Sensor FOV was varied from ±10° to ±90° and sensor range was varied from 20m to 100m. Sensor range had a negligible effect on the estimated pedestrian detection capability, but a longer range did increase the length of time the pedestrian was visible. Wider sensor FOV resulted in higher pedestrian detection capability. The narrowest sensor could potentially detect an estimated 58% of pedestrians whereas the widest sensor was estimated to detect up to 99% of the pedestrians.

Keywords **Pedestrian detection, Automatic Emergency Braking, PCDS, United States, Simulation**

I. INTRODUCTION

Automatic Emergency braking (AEB) systems have the potential to mitigate or avoid vehicle-pedestrian crashes, if they can detect pedestrians with sufficient time to take evasive action. Many studies have estimated the potential effectiveness of AEB for avoiding and mitigating vehicle pedestrian crashes using European datasets such as the German In-Depth Accident Study (GIDAS). Rosén, Kallhammer [1] simulated GIDAS vehicle-pedestrian crashes with a variety of sensor Field-of-views (FOVs) and estimated that AEB could reduce fatal injuries by a maximum of 67.7%. Gruber, Kolk [2] conducted a similar analysis on three European databases and estimated avoidance effectiveness values for pedestrian AEB systems was between 39.5% and 79.4% depending on the dataset and system parameters.

While these studies are useful for evaluating vehicle-pedestrian crashes in Europe, their results may not be representative of US vehicle-pedestrian crashes due to differences in pedestrian infrastructure, vehicle infrastructure, laws and enforcement, rates of impaired and distracted driving, vehicles, and vehicle usage rates [3]. The US fleet has a larger proportion of light trucks and vans (LTVs) than European fleet which has an effect on injury outcomes. Lefler and Gabler [4] found that fatal injuries were 2 to 3 times more likely when pedestrians were struck by LTVs than when pedestrians were struck by passenger cars.

The US has limited in-depth vehicle-pedestrian crash data which makes simulating these crashes difficult. Haus, Sherony [5] used the pedestrian crash data study (PCDS) and estimated that the vehicle-pedestrian crash avoidance system potential could be as high as 86% assuming the system had no FOV or range limitations. Combs, Sandt [6] estimated the effectiveness of automated vehicles to be between 36% and 98% by using the Fatality Analysis Reporting System (FARS) and assumed sensor limitations in various scenarios such as adverse weather conditions. FARS is a census of all the pedestrian fatalities that occur on U.S. public roads each year [7]. While FARS is a valuable resource, it does not contain important in-depth data, such as the positions of the pedestrian and striking vehicle, estimated impact speeds, or detailed crash scene diagrams, necessary to simulate real-world crashes.

The objective of this study was to examine the effect of AEB sensor FOV and range on the detection of pedestrians in real-world US vehicle-pedestrian crashes using PCDS.

S. H. Haus is a PhD candidate in Biomedical Engineering at Virginia Tech in Virginia, USA (shaus@vt.edu). R. Sherony is a Sr. Principal Engineer at the Collaborative Safety Research Center (CSRC), Toyota Motor North America in Ann Arbor, Michigan, USA. H. C. Gabler is Professor of in the Department of Biomedical Engineering and Mechanics at Virginia Tech in Virginia, USA.

II. METHODS

Vehicle-pedestrian crashes were reconstructed to create vehicle and pedestrian trajectories. The crashes were then simulated with various hypothetical AEB sensor systems to estimate each sensor system's pedestrian detection ability.

Data Sources

This study used vehicle-pedestrian crashes from the Pedestrian Crash Data Study (PCDS). PCDS was collected from 1994 to 1998 by the National Highway Traffic Safety Administration (NHTSA) using a modified method from the National Automotive Sampling System Crashworthiness System Study (NASS-CDS). The data set contains 530 crashes involving 549 pedestrians. To be included in the dataset, the vehicle had to be moving forward, strike the pedestrian in front of the A-pillar, and involve a late model vehicle (manufactured within five years of the collection year) in which the pedestrian was not sitting or lying down [8]. Each case included detailed information on the crash, environmental characteristics, vehicle damage, and Abbreviated Injury Scale (AIS) coding of pedestrian injuries (AIS90). In addition, each crash had a scaled scene diagram of the environment which included the pre-impact locations of the pedestrian and striking vehicle. If possible, the crash scene investigator reconstructed the impact speed of the striking vehicle [9]. For this study, only cases with frontal damage and reconstructed impact speeds were included resulting in a total of 357 cases.

PCDS is the only publicly available U.S. dataset with this depth of information for vehicle-pedestrian crashes making it a valuable resource for simulating U.S. vehicle-pedestrian crashes. Unfortunately, the PCDS study design did not calculate case weights to be able to relate the crashes to nationwide incidence. Therefore, a weighting scheme, based on the distribution of crashes in the National Automotive Sampling System (NASS) – General Estimates System (GES), was developed to relate the PCDS vehicle-pedestrian crashes to the modern incidence of these crashes. NASS-GES was a probability sample of all police-reported crashes in the U.S. and was collected by NHTSA from the 1988 to 2015. GES does not contain crash scene diagrams or reconstruction and did not use AIS coding to report injuries [10]. The PCDS case weight was based on if the pedestrian was a child (<15) or adult, if the vehicle was a car or LTV, and the reported injury severity. These metrics were chosen because PCDS over-sampled cases with children and higher severity injuries. In addition, due to the age of the dataset, the sample's fleet could have a higher proportion of sedans than the current US fleet. Police reported injury, reported on the KABCO scale, was used as a surrogate for AIS injury coding as GES does not record specific injuries or the AIS severity [11]. The weighting factors were calculated by dividing the proportion of GES pedestrian crashes from 2011 to 2015 in each category by the proportion of PCDS crashes in each category. Table 1 shows the weighting factors used. A value of NA indicates that there were no PCDS cases in that category.

TABLE I
Weighting Factors for PCDS by pedestrian age, striking vehicle type, and police reported injury severity (KABCO scale)

		Child (<15)		Adult (≥15)	
	Striking Vehicle Type	Car	LTV	Car	LTV
KABCO Scale	O – No injury	0.474	0.929	2.974	3.896
	C – Possible Injury	0.852	1.866	1.739	1.732
	B – Non-incapacitating Injury/ Suspected Minor Injury	0.734	1.026	1.435	1.326
	A – Incapacitating Injury/ Suspected Serious Injury	0.285	0.842	0.594	0.724
	K - Killed	0.718	NA	0.367	0.532
	U – Injury, Unknown	0.240	NA	0.513	0.618

A chi-square goodness of fit analysis was conducted to compare the distributions of pedestrian, environmental, and pre-crash characteristics in PCDS to the distributions of variable in the NASS-GES database over the 2011 to 2015 time span. The unweighted PCDS data had significantly different distributions for all the examined variables except for pedestrian gender. The weighted PCDS data was an improvement over the unweighted data in that it did not have significantly different distributions of pedestrian gender, weather conditions, and pre-event vehicle movement. Significance was determined using a confidence level of 0.05.

Reconstruction

To reconstruct the vehicle and pedestrian trajectories, the trajectory points were digitized from the scanned PCDS crash scene diagrams. The scene diagrams were loaded into AutoCAD, scaled, and orientated so that origin was located at the front centre of the vehicle at impact with the vehicle heading toward the positive y-axis. The vehicle and pedestrian trajectory points were then collected relative to the origin. If a crash scene diagram only had one vehicle trajectory point, a second trajectory point was extrapolated based on the impact position of the vehicle, vehicle heading, and the event summary. To create a smooth vehicle/pedestrian path, the measured trajectory points were connected together. If the trajectory was straight, a linear path was fit to the trajectory points using linear regression to minimize the error of the positions in the scene diagram. For curved trajectories, the measured trajectory points were fit to a curve. To fit the curved trajectories, the trajectory points were loaded into MATLAB and the curve fitting tool was used to fit the points, minimizing the root mean square error, with a variety of potential curve models including, but not limited to, exponential, power, tangent, cotangent, and secant. Two cases, where the vehicle/pedestrian was performing a "U-turn" manoeuvre, were fit using a parabolic model. The models were manually inspected to ensure that they fit with the crash summary and then the model with the best R-squared value was used. The vehicle and pedestrian trajectories are shown in Fig. 1 and Fig. 2 in global coordinates, where the origin was the front and centre of the vehicle, the y-axis was along the vehicle longitudinal axis, and the x-axis was along the vehicle's front bumper, all at the point of impact.

To obtain the position and speed of the vehicle and pedestrian in the time prior to the crash, the scenario was reconstructed backwards from the point of impact based on the impact speed estimated by the crash scene investigator. The pedestrian was assumed to walk at a constant speed and take no evasive actions. Pedestrian speed was predicted based on the pedestrian's age and whether or not they were travelling in a group. The pedestrian walking speed ranged from 1.15 to 1.45 m/s based on the pedestrian age and whether or not they were walking in a group [12]. For the vehicle, if there was no evidence that the driver braked before the collision, it was assumed that the vehicle travel speed was equivalent to the impact speed. If there was evidence of braking, there were two equally likely potential driver braking patterns utilized, an early and weak braking pattern and a late and hard braking pattern. The early/weak braking driver pattern was assumed to start braking at a time-to-collision (TTC) of 2 seconds with a maximum deceleration of 0.2 g. The late/hard braking driver pattern was assumed to start braking at a time-to-collision (TTC) of 0.4 seconds with a maximum deceleration of 0.4 g. These two braking models were chosen because the true brake timing and maximum deceleration were not known. The two braking models were intended to represent an upper and lower bound with the driver's true braking profile falling within the bounds [13]. Both braking models were assumed to have a jerk, or acceleration rate, of 10.7 m/s^3. If there was braking, the braking was assumed to begin at the TTC value of the braking model whether or not the pedestrian was visible and in the road. The vehicle and pedestrian trajectories were calculated out to a TTC of 3 seconds.

For each time point we also recorded whether or not the pedestrian was in the road and whether or not the pedestrian was obstructed from the drivers' view. For this study, only physical obstructions, such as parked and moving cars and any physical objects denoted in the crash scene diagram, were considered. Visual obstructions such as glare from the sun or headlights were not considered. Similarly, darkness or lack of street lighting were not considered obstructions for this study.

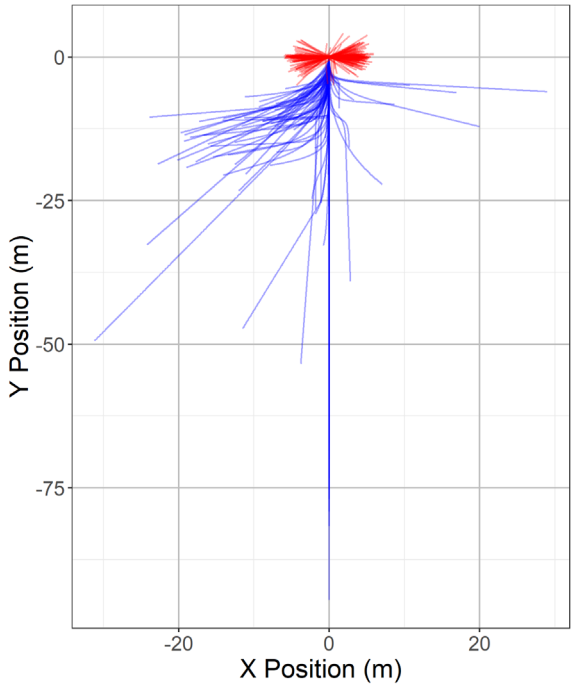

Fig. 1. Early/weak braking driver trajectories in global coordinates. Vehicle trajectories in blue and pedestrian trajectories in red.

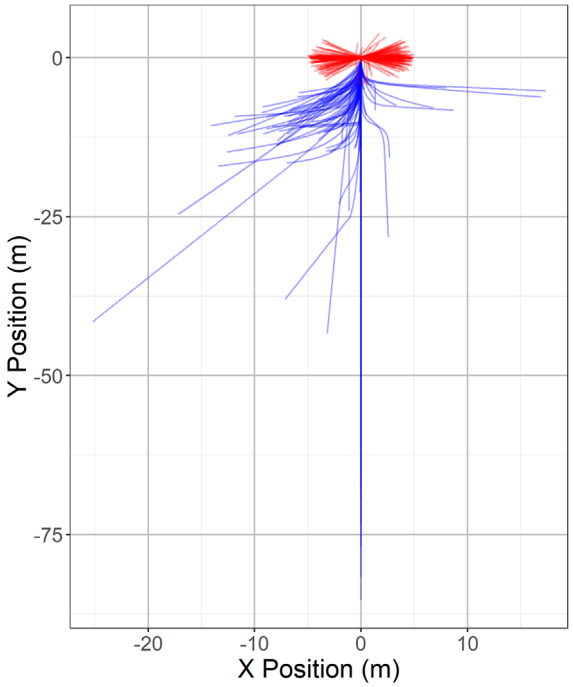

Fig. 2. Late/hard braking driver trajectories in global coordinates. Vehicle trajectories in blue and pedestrian trajectories in red.

Simulation

Based on the calculated vehicle and pedestrian trajectories, simulations were conducted with a hypothetical AEB model to estimate when and where various hypothetical AEB sensors could potentially detect the pedestrians. The AEB sensor was modelled on the front centre edge of the vehicle with varied sensor field-of-view (FOV) and ranges. It was assumed that the sensor was attached to the front and centre of the vehicle with the centre axis of the FOV aligned with the longitudinal axis of the vehicle. FOV was varied from ±10° to ±90° and range was varied from 20 m to 100 m to capture a range of system specifications seen in commercially available radar and LiDAR systems [14].

The simulation was conducted using a specially developed code written in the R programming language. The code used the vehicle and pedestrian trajectories to determine the starting parameters and the path the vehicle and pedestrian would take and then it iterated forward in time. At each time point the code determined if the pedestrian was detectable based on their location relative to the vehicle, whether they were in the road, and whether they were obstructed from the sensor's view. If the pedestrian's location was within the range and FOV of the sensor and there was a direct line of sight to the pedestrian; then it was assumed that the pedestrian was detected by the sensor. This assumed that the sensor system, regardless whether radar, LiDAR, or cameras, was always capable of detecting a pedestrian in view. We assumed that an AEB system would only detect a pedestrian once it was in the road because if the pedestrian was not in the roadway, it was assumed that the system would not perceive the pedestrian as a threat.

At every time point, the code used the kinematic equations of motion to calculate the displacement over the time step (0.01 seconds) and the new velocity and acceleration for the vehicle and pedestrian. The displacement was projected onto the estimated path to calculate the new vehicle and pedestrian location. It was assumed that the front and centre of the vehicle followed the estimated path. A simple bicycle type kinetic model was used to calculate the location of the vehicle rear relative to the vehicle front. For this study, the primary focus was pedestrian detection and not on avoidance/mitigation, therefore the hypothetical AEB system was designed to not activate. More details on the full code can be found in Haus, Sherony [15].

Analysis was conducted by identifying whether or not the pedestrian could be detected prior to impact, the pedestrian's location relative to the hypothetical AEB system at the time of detection, and the time-to-collision (TTC) at the time of detection. The pedestrian's relative location was calculated relative to the AEB system on the vehicle meaning that the y-axis corresponds to the centre forward facing axis of the sensor. The TTC at detection

was calculated by dividing the linear distance to the original impact point by the vehicle speed at the moment the pedestrian was detected. In addition, the relative location of the pedestrian was calculated at TTCs of 1, 2, and 3 seconds to examine the sensor angle and range necessary to detect pedestrians over time.

III. RESULTS

Sensor effectiveness was first defined as the ability of the sensor to detect the pedestrian before impact. As shown in Fig. 3, sensor range had very little effect on the ability for the sensor to detect the pedestrian. Only the sensor with a FOV of ±10° showed any effect of sensor range with a 3 percentage point decrease in estimated detection ability for a sensor with a 20 m range compared to a range of 40 m or greater. Sensor FOV had a larger effect on the ability of the system to detect the pedestrians. The sensor with the narrowest FOV (±10°) was able to detect an estimated 58-61% of the pedestrians while the widest FOV sensor (±90°) was able to detect 99% of the pedestrians.

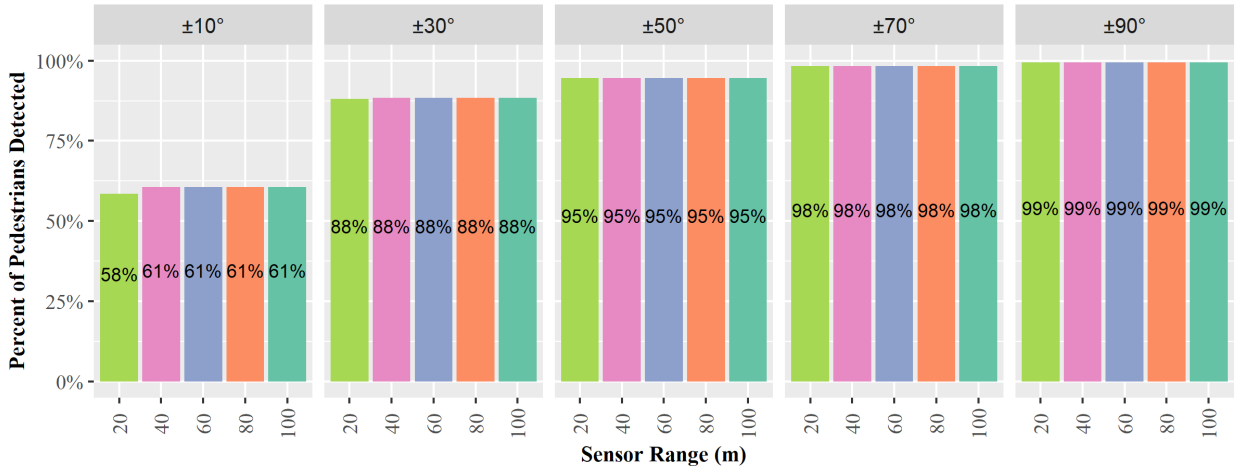

Fig. 3. Percentage of cases in which the pedestrian was detected for sensor FOVs from ±10° to ±90° and sensor ranges from 20m – 100m.

While sensor range did not show a large effect on the ability to detect a pedestrian before impact it does have a substantial effect on where the pedestrian was detected. As shown in Fig. 4, the AEB system with the narrower FOV and shorter range detected the pedestrian much closer to the impact point. While the pedestrian is still detected with a shorter range sensor, the system would have much less time to detect, identify, and take evasive action to avoid the collision. Also notable is that even when the FOV is wide and the range is long, many pedestrians were not detected until they were within 50 m and only a few were detectable at distance greater than 80 m. As expected, cases in which there were obstructions (Fig. 4 blue points), the pedestrian tended to be detected much closer to the impact point than cases with no known obstructions.

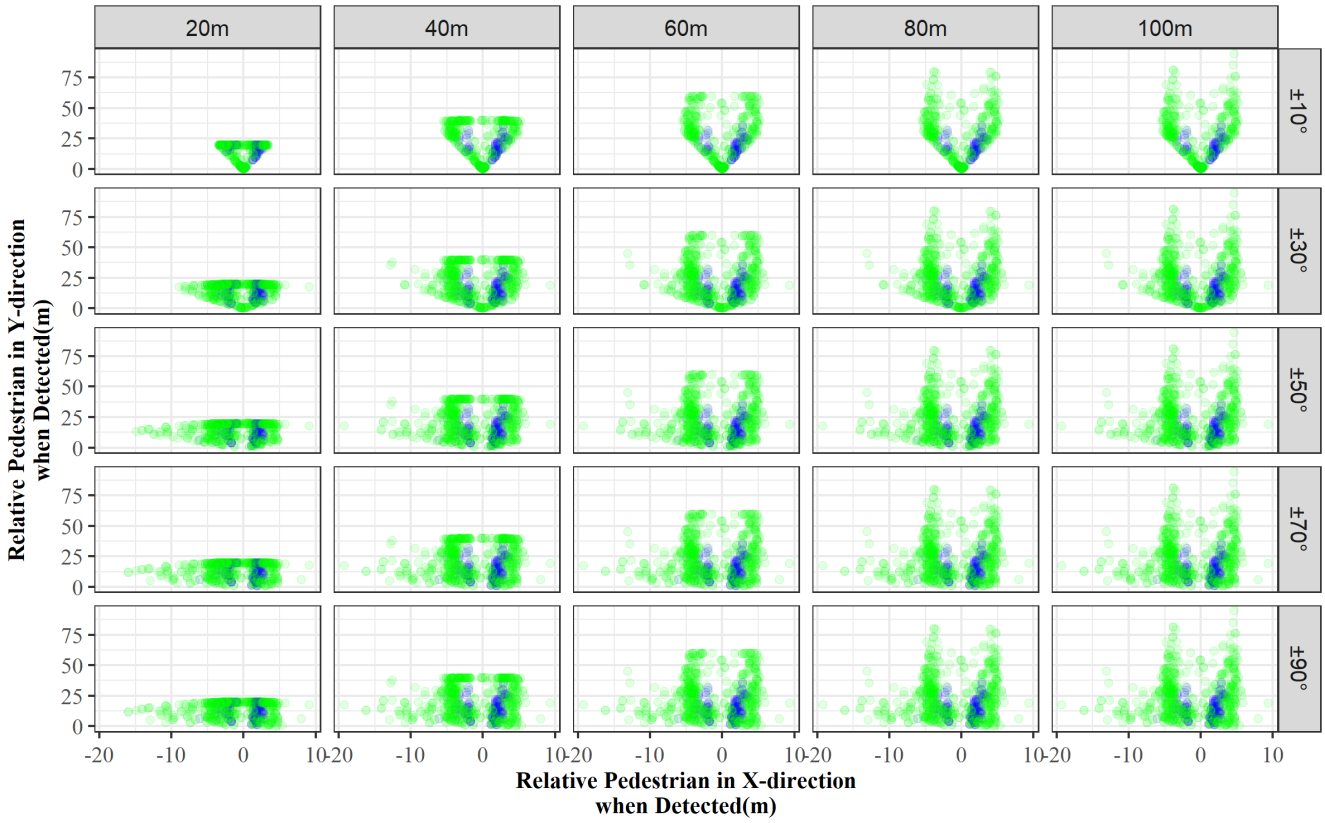

Fig. 4. Pedestrian location when first detected by sensor system with sensor FOVs from ±10° to ±90° and sensor ranges from 20m – 100m. Blue points indicate cases with obstructions and green points indicate cases with no known obstruction.

The pedestrian's location when detected can indicate the urgency of the situation, but it was difficult to determine how much time the system would have to react by that metric alone because the vehicle speed was not taken into account. To account for speed the TTC was calculated at the time the pedestrian was detected. As shown in Fig. 5, in less than 25% of the cases the pedestrian was estimated to be detectable at TTCs less than 1 second. The median TTC at detection increased with increasing sensor FOV and range. Increasing sensor FOV primarily increased the toe region of the graph so that there were fewer cases with a TTC of less than 1 second at detection. Increasing sensor range primarily increased the number of pedestrians that were detectable at the maximum TTC of 3 seconds. A TTC of 3 seconds was the most common detection which indicates that many pedestrians were detected at the start of the simulation. It is possible that the pedestrians could have been detected at TTCs higher than 3 seconds, but longer TTCs were not considered in this study.

The relative pedestrian angle and distance was examined at TTCs of 1, 2, and 3 seconds (Fig. 6 and Fig. 7). As expected, median pedestrian distance decreased with TTC. The median distance at a TTC of 1 second was 6.4 m compared to median distances of 15.5 m and 22.4 m for TTC of 2 and 3 seconds, respectively. There was very little difference between the relative pedestrian angles across TTC, although angles decreased slightly as TTC increased. The median pedestrian angle was 14.3°, 12.5°, and 11.5° for a TTC of 1,2, and 3 seconds, respectively.

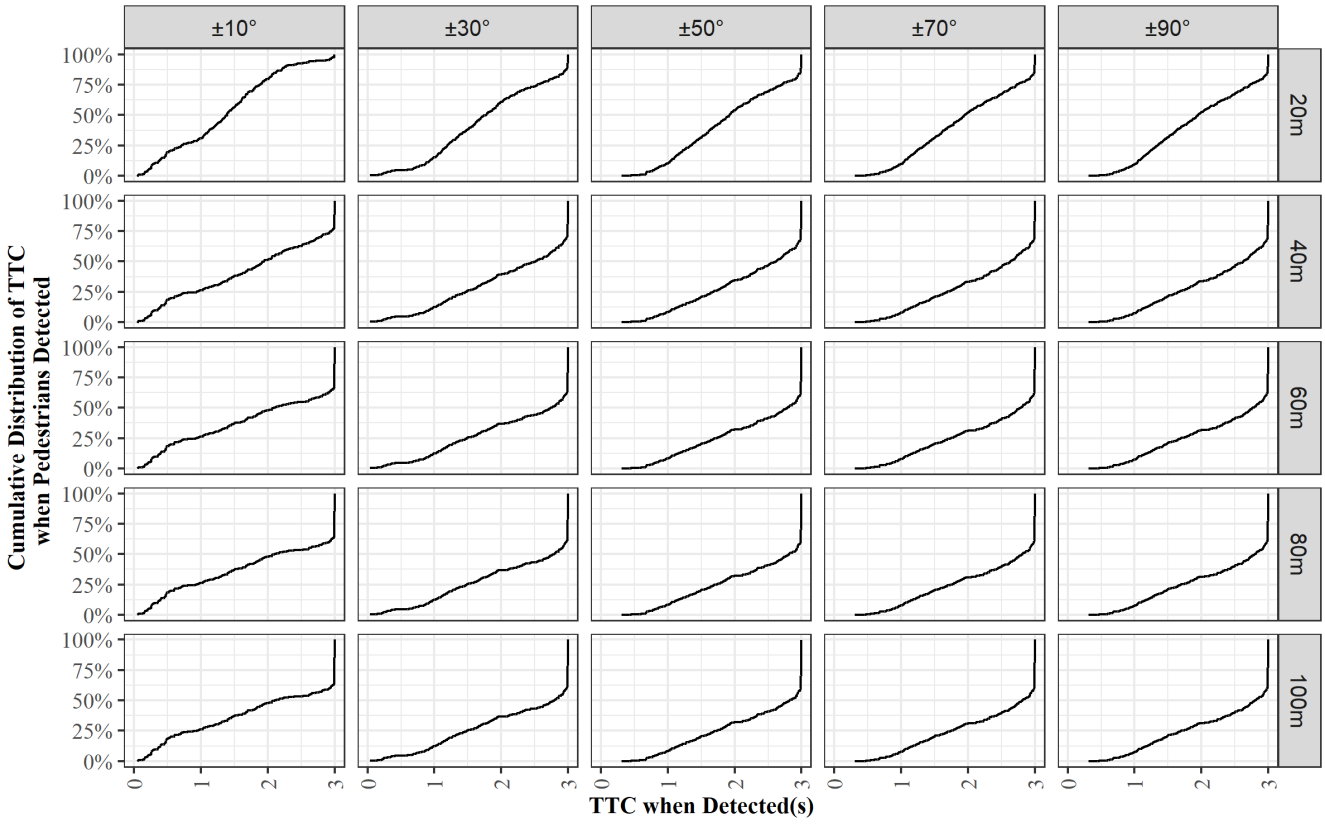

Fig. 5. Cumulative distribution of TTC at pedestrian detection by sensor system with sensor FOVs from ±10° to ±90° and sensor ranges from 20m – 100m.

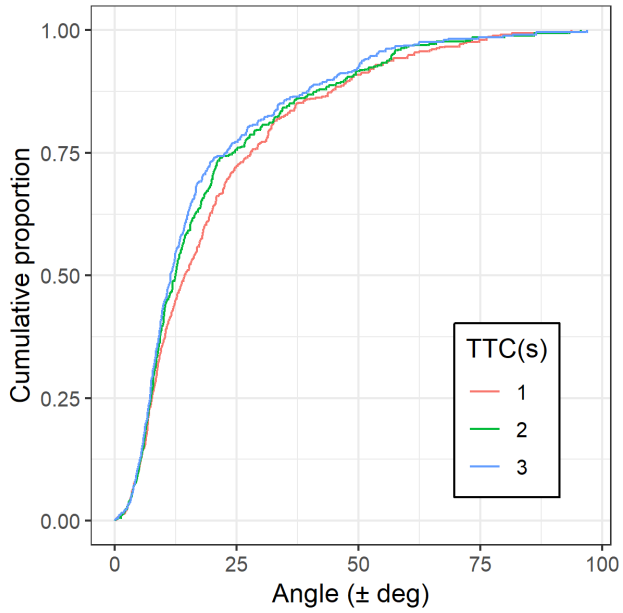

Fig. 6. Cumulative distribution of pedestrian angle relative to hypothetical AEB system at a TTC of 1 (red), 2 (green), and 3 (blue) seconds.

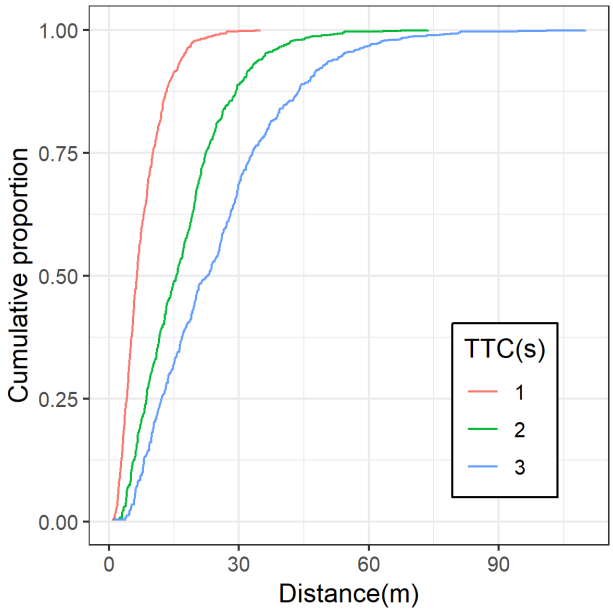

Fig. 7. Cumulative distribution of pedestrian distance relative to hypothetical AEB system at a TTC of 1 (red), 2 (green), and 3 (blue) seconds.

IV. DISCUSSION

In-depth vehicle-pedestrian crash data in the U.S. is limited. While PCDS is the most recent publicly available vehicle-pedestrian crash database that contains reconstructions, crash scene diagrams, detailed vehicle damage reports, and detailed injury records, the age and size of the dataset is a limitation. The data set was collected

from 1994 to1998 and contains only 530 crashes. While we assumed that the crashes from the collection range resemble crashes that occur today, changes in driver or pedestrian behaviour, different types of distractions, and more pedestrian friendly intersections could affect the applicability of these crashes.

The simulation model assumed that the vehicle followed the estimated trajectory and that the vehicle was able to achieve the necessary braking regardless of the lateral acceleration associated with turning. Given the hypothetical braking forces used in this study did not exceed 0.4 g, we believe this is a good assumption, but this assumption may not be so applicable with higher braking forces.

Time to collision (TTC) was calculated by the linear distance to the impact point by the vehicle velocity. While this assumption is good for cases in which the vehicle is travelling straight, this method may underestimate the TTC for vehicles in turning cases, particularly at longer TTCs.

The sensor with the widest FOV was estimated to be able to detect 99% of pedestrian before the crash occurred. This estimate assumed an ideal sensor i.e. a sensor that had no false positive or false negatives, was equally effective in all weather and lighting conditions, and instantly detected the pedestrian. Studies have shown that different sensors, such as camera, radar, and LiDAR may have different effectiveness based on the distance of the pedestrian, environmental conditions, and pedestrian characteristics such as height or clothing type [16]. AEB systems may also have a computational latency over which the system must identify that the pedestrian is a pedestrian and that they are on a trajectory to interact with the vehicle. These factors were not considered in this study and may reduce the detection ability of a sensor system.

In addition, we assumed the sensor was located on the front centre of the vehicle. If the pedestrian became visible immediately prior to the crash the sensor cone may have missed the pedestrian. Alternate sensor placement or additional sensors, such as corner sensors, could affect the ability for the system to detect the pedestrians in these cases, but that was not examined in this study.

This work only considered pedestrian detection. While sensor FOVs above 70° showed minimal additional detection benefit in this study, wider FOV sensors may benefit other vulnerable road users such as bicyclists. Lenard, Welsh [17] found that bicyclists required wider FOVs and longer ranges to be detected in the same proportions as pedestrians. US studies have examine earliest detection opportunity for bicyclist and animals [18] [19], but have not to our knowledge conducted analysis of sensor requirements necessary to detect these other road users.

The results presented in this study generally agree with similar analysis conducted using European data. Lenard, Welsh [17] conducted a TTC analysis of pedestrian crashes using in-depth data from the UK and found similar distributions of distances at the TTCs leading up to the crashes, but a smaller range of pedestrian angles. Lenard, Welsh [17] did not show pedestrian angles above ±45°, whereas this study shows angles as high as ±90° despite both datasets containing cases with travelling straight and turning vehicles.

V. CONCLUSIONS

The objective of this study was to examine the effect of AEB sensor field-of-view (FOV) and range on the detection of pedestrians in real-world US vehicle-pedestrian crashes. Sensor range was found to have only a small effect on the overall number of pedestrians detected. However, increasing the sensor range increased the TTC at which the pedestrian was detected which would provide more time for an AEB system to avoid or mitigate the impact. Sensor FOV was estimated to have a larger effect on the ability of a sensor to detect a pedestrian before impact than the sensor range. Sensor FOV was also estimated to have a positive effect on the TTC when detected, with wider FOVs resulting in fewer cases with a TTC of detection under 1 second. AEB systems that detect a pedestrian with less than one second TTC might have difficulty avoiding the collision. The more time an AEB system has, the greater the potential to avoid or mitigate a crash.

VI. ACKNOWLEDGEMENT

The authors would like thank the Toyota Collaborative Safety Research Center for funding this study and Jordan Moon, an undergraduate research assistant, for her assistance digitizing the vehicle and pedestrian trajectories.

VII. REFERENCES

[1] Rosén, E., Kallhammer, J.E., et al. Pedestrian injury mitigation by autonomous braking. *Accident Analysis and Prevention*, 2010. 42(6): p. 1949-1957

[2] Gruber, M., Kolk, H., et al. The Effect of P-AEB System Parameters on the Effectiveness for Real World Pedestrian Accidents. *Proceedings* 2019.
[3] Buehler, R. and Pucher, J. The growing gap in pedestrian and cyclist fatality rates between the United States and the United Kingdom, Germany, Denmark, and the Netherlands, 1990–2018. *Transport Reviews*, 2021. 41(1): p. 48-72
[4] Lefler, D.E. and Gabler, H.C. The fatality and injury risk of light truck impacts with pedestrians in the United States. *Accident Analysis & Prevention*, 2004. 36(2): p. 295-304
[5] Haus, S.H., Sherony, R., and Gabler, H.C. Estimated benefit of automated emergency braking systems for vehicle–pedestrian crashes in the United States. *Traffic Injury Prevention*, 2019. 20(sup1): p. S171-S176
[6] Combs, T.S., Sandt, L.S., Clamann, M.P., and McDonald, N.C. Automated Vehicles and Pedestrian Safety: Exploring the Promise and Limits of Pedestrian Detection. *American Journal of Preventive Medicine*, 2019. 56(1): p. 1-7
[7] National Highway Traffic Safety Administration. Fatality Analysis Reporting System (FARS) Analytical User's Manual (1975-2017) 2018
[8] Chidester, A.B. and Isenberg, R. FINAL REPORT - THE PEDESTRIAN CRASH DATA STUDY. *Proceedings* 2001.
[9] NHTSA. Pedestrian Crash Data Study 1996 Data Collection, Coding, and Editing Manual. 1996: Washington.
[10] National Highway Traffic Safety Administration. National Automotive Sampling System General Estimates System analytical user's manual, 1988-2015. 2018: Washington, DC.
[11] MMUCC Guidline: Model Minimum Uniform Crash Criteria, D.o. Transportation, Editor. July 2012. p. 631.
[12] Gates, T.J., Noyce, D.A., Bill, A.R., and Van Ee, N. Recommended Walking Speeds for Pedestrian Clearance Timing Based on Pedestrian Characteristics. *TRB Annual Meeting*, 2006
[13] Kusano, K.D. and Gabler, H.C. Safety Benefits of Forward Collision Warning, Brake Assist, and Autonomous Braking Systems in Rear-End Collisions. *IEEE Transactions on Intelligent Transportation Systems*, 2012. 13(4): p. 1546-1555
[14] System Reference document (SRdoc); Transmission characteristics; Technical characteristics for radiodetermination equipment for ground based vehicular applications within the frequency range 77 GHz to 81 GHz. 2020.
[15] Haus, S.H., Sherony, R., and Gabler, H.C. Differential Benefit of LiDAR and Current Sensor Systems in Pedestrian Automated Emeregency Braking Systems. *Traffic Injury Prevention*, 2021. In Press
[16] Mohammed, A.S., Amamou, A., et al. The Perception System of Intelligent Ground Vehicles in All Weather Conditions: A Systematic Literature Review. *Sensors (Basel, Switzerland)*, 2020. 20(22): p. 8-22
[17] Lenard, J., Welsh, R., and Danton, R. Time-to-collision analysis of pedestrian and pedal-cycle accidents for the development of autonomous emergency braking systems. *Accident Analysis & Prevention*, 2018. 115: p. 128-136
[18] Haus, S.H., Anderson, R.M., Sherony, R., and Gabler, H.C. Potential Effectiveness of Bicycle-Automatic Emergency Braking using the Washtenaw Area Transportation Study Data Set. *Transportation Research Record*, 2021
[19] Decker, J.A., Haus, S.H., Sherony, R., and Gabler, H.C. Potential Benefits of Animal-Detecting Automatic Emergency Braking Systems Based on U.S. Driving Data. *Transportation Research Record*, 2021: p. 03611981211012416